JOURNAL OF MATERIALS SCIENCE **39** (2004) 4095–4101

Formation of intergranular amorphous films during the microstructural development of liquid phase sintered silicon carbide ceramics

E. VOLZ, A. ROOSEN*
Institute of Glass and Ceramics, Department of Materials Science, University of Erlangen-Nuremberg, Martensstrasse 5, 91058 Erlangen, Germany
E-mail: roosen@ww.uni-erlangen.de

S.-C. WANG, W.-C. J. WEI
Institute of Materials Science and Engineering, National Taiwan University, 1 Roosevelt Rd. Section 4, 106, Taipei, Taiwan, Republic of China

The microstructure of liquid phase sintered SiC ceramics was characterised by means of high resolution transmission electron microscopy (HRTEM). The SiC ceramics were pressureless sintered with the additions of Al_2O_3 and Y_2O_3 at sintering temperatures of 1800 and 1950°C, respectively. At a sintering temperature of 1800°C the microstructure of the SiC ceramics has no crystallised secondary phase and the SiC grains are separated by an intergranular amorphous film. In contrast, in the case of the microstructure of SiC ceramics sintered at 1950°C a clean interface without any amorphous layer between the SiC grains was observed. The secondary phase is crystallised into the $Y_3Al_5O_{12}$ phase and exhibits a clean interface between the SiC grains. An explanation for the existence or the absence of the intergranular glass films are given by an extended Clarke's model of the force balance of attractive van der Waals forces and repulsive steric forces. The chemical decomposition of the intergranular glass film at elevated temperature was considered.

1. Introduction

Silicon carbide (SiC) ceramics are used as a structural material for high temperature and mechanical applications due to its high oxidation resistance and fracture strength at elevated temperatures, excellent thermal conductivity and low coefficient of thermal expansion. These outstanding properties have their origin in the strong covalent bonding character. The high amount of covalent bond results in low selfdiffusion coefficients. Therefore it is not possible to sinter pure SiC without high pressure [1]. Prochazka was the first who sintered SiC pressureless with additions of boron and carbon via a solid-state-sintering mechanism up to 98% of theoretical density (TD) at temperatures around 2200°C [2]. 15 years later other authors [3–5] demonstrated the possibility of pressureless sintering of SiC in a temperature range between 1850 and 2000°C with the additions of Al_2O_3 and Y_2O_3 via the formation of a liquid phase. After that, research has focused on improving the mechanical properties of SiC [6–9]. Many investigations have been carried out to study kinetics of the microstructural development in liquid-phase-sintered (LPS) SiC ceramics [10, 11], specifically about the structure of grain boundary interfaces and intergranular amorphous films. Some authors observed amorphous layers at the grain boundary interface [12–15]. But also clean interfaces had been reported, which did not show any separating amorphous layer [16–18]. Different factors seem to be responsible for the stability or instability of the grain boundary films.

The aim of this paper is to study the microstructural development of liquid phase sintered SiC ceramics at different sintering stages with the focus on the characterisation of the intergranular amorphous film formation by means of Transmission Electron Microscope (TEM) and High Resolution Transmission Electron Microscope (HRTEM) investigations. Also the crystallisation of the secondary phase in these SiC ceramics was observed. These results support the interpretation of the electron conductivity behaviour of LSP SiC ceramics which will be published in another paper.

2. Experimental procedure

SiC ceramics had been prepared via dry pressing and liquid phase sintering. As a starting powder a commercial Acheson α-SiC powder (Grade UF-25, H. C. Starck, Goslar, Germany) was used with a specific

*Author to whom all correspondence should be addressed.

surface area of 25 m^2/g (Micromeritics, Typ ASAP 2000, Norcross, GA, USA) and a d_{50} value of 0.5 μm (Mastersizer 2000, Malvern Instruments Ltd., UK). 10 vol% of the sintering additives Al_2O_3 (A 16 SG, Alcoa Coorp., USA) and Y_2O_3 (OX39-5N, Stanford, San Mateo, USA) in the molar ratio of 3:5 were added to the starting powder to promote liquid phase sintering. The powder mixture was homogenised in an attrition mill with SiC grinding media in isopropanol for 4 h. After homogenisation the slurry was separated from the grinding media and the isopropanol was evaporated. Green bodies were produced without the addition of binder by cold uniaxial pressing at a pressure of 125 MPa. The pressed pellets were placed inside a closed graphite crucible. The crucible was filled with a loose SiC powder bed. At the bottom and at the top the SiC powder was covered by a layer of Al_2O_3 powder. Pressureless sintering was performed in a graphite resistance furnace (FCT Anlagenbau GmbH, Typ FSW 200/250-2200-PS/TS, Sonneberg, Germany) in a flowing argon atmosphere at a heating and cooling rate of 10°C/min. The sintering temperature was varied between 1800 and 1950°C with a holding time of 30 min.

After firing the linear shrinkage of the sintered samples was determined and the density was measured by the Archimedes method. According to the rule of mixtures the theoretical density of the samples was calculated to be 3.335 g/cm^3. TEM specimens were prepared by the standard techniques cutting, grinding, ultrasonic drilling, dimpling, polishing and Ar-ion beam milling. The transmission electron microscope (HRTEM, Philips CM300 Technai, Netherlands) was used to characterise the microstructure of the liquid phase sintered SiC ceramics.

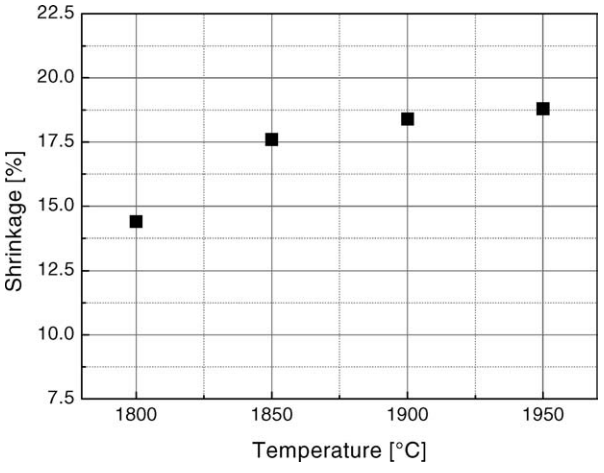

Figure 1 Linear shrinkage of the LPS SiC specimens at different sintering temperatures (10 vol% sintering additives).

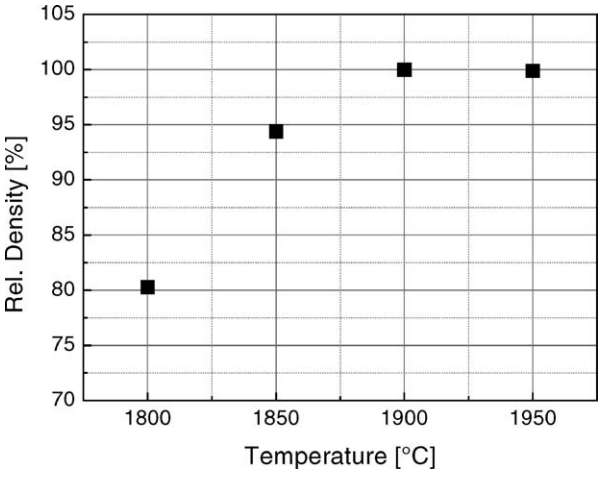

Figure 2 Density of the LPS SiC specimens as a function of sintering temperature (10 vol% sintering additives).

3. Results

The densification mechanism of SiC ceramics doped with the additions of Al_2O_3 and Y_2O_3 is generally attributed to liquid phase sintering by means of a solution-precipitation process. The additions form a liquid phase at the eutectic temperature of about 1760°C [19]. The silica which is located on the surface of the SiC grains decreases the eutectic temperature of the liquid phase [19]. Fig. 1 shows the amount of shrinkage of liquid phase sintered SiC ceramics in the temperature range between 1800 and 1950°C. The shrinkage increases from 14.4 to 18.8% with increasing sintering temperature. In the investigated temperature range the SiC grains are wetted by the liquid phase, which is formed by the added sintering additives. At higher sintering temperature the viscosity of the liquid phase decreases and promotes the transport rate of SiC in the liquid phase and also the reorientation of the grains by capillary forces.

Fig. 2 shows the relative density of the sintered SiC ceramics in dependence of the sintering temperature. The SiC ceramics exhibit a density of 80% TD and consequently a porosity of 20% at a sintering temperature of 1800°C. With enhanced sintering temperature of 1900°C the SiC ceramics show a rapid increase of the density up to the theoretical density. At higher temperatures the density increases slower and the liquid phase sintered SiC ceramics become fully dense.

3.1. Microstructure of SiC ceramics sintered at 1950°C

Fig. 3 shows a TEM micrograph of the typical microstructure of LPS SiC at a temperature of 1950°C. In the microstructure there is no porosity. The brighter areas are SiC grains. The stripes in the bright SiC grains are caused by typical staking faults in the SiC lattice. The diffraction patterns of the SiC grains did not show a preferred orientation of the crystal lattice of the individual SiC grains. The dark intergranular phase is a crystalline structure. The electron diffraction pattern of the secondary phase is shown on the right top of the TEM micrograph. The determined d-value from this pattern indicates the cubic crystal lattice of the $Y_3Al_5O_{12}$ (YAG)-phase. Energy dispersive X-ray spectroscopy (EDX) of the secondary phase in the triple points resulted in a ratio of aluminium to yttrium of 4.47:2.03. This ratio corresponds almost to the molecular ratio of aluminium to yttrium in the YAG phase, which crystallised from the liquid phase during the cooling process. Electron diffraction by means of

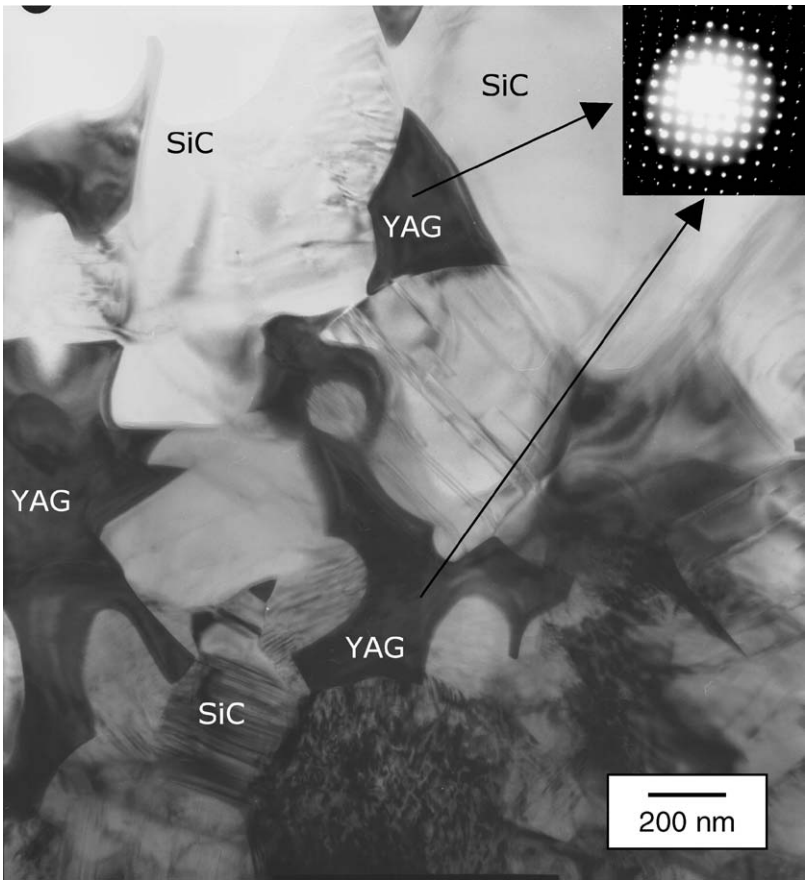

Figure 3 TEM micrograph of a SiC ceramic sintered at a temperature of 1950°C (top figure: diffraction pattern of the secondary phase).

TEM of the intergranular phase shows that the YAG phase exhibits a congruent crystallographic orientation over larger areas and in neighbouring pockets. Under the assumption of a connected secondary matrix phase in which several SiC grains are embedded the taken diffraction patterns must be from one and the same YAG crystal. This observation is consistent with other reports in the literature [13].

The occurring interfaces in the microstructure of dense LPS SiC ceramics sintered at a temperature of 1950°C are shown in Fig. 4. The HRTEM image A shows the interface between a SiC grain and the crystallised secondary phase. The lattice fringes in the SiC grain have a spacing of 0.217 nm. The crystallised YAG phase exhibits a spacing of the lattice fringes of 0.58 nm which corresponds to the 210 plane. The interface of the two grains does not show any amorphous structure, and no separating layer between the different crystal lattices can be detected. The interface between two SiC grains is shown in picture B. One lattice of the SiC grain is orientated along the *c*-axis and has a stacking plane sequence of 6 layers. These 6 layers have the typical width of 0.152 nm which corresponds with the 6H-SiC polytype. The interface between the SiC grains is also clean and exhibits no intergranular amorphous film. The different orientated lattices of the SiC grains are in direct contact with each other at the grain boundaries.

3.2. Microstructure of SiC ceramics sintered at 1800°C

Fig. 5 shows a typical TEM image of the microstructure of the pressureless sintered specimen at a sintering temperature of 1800°C. The microstructure contains pores (bright areas) and round SiC grains (darker areas). The specimen has approx. 20% porosity, because the sintering temperature of 1800°C was insufficient for a complete densification. A secondary phase consisting of

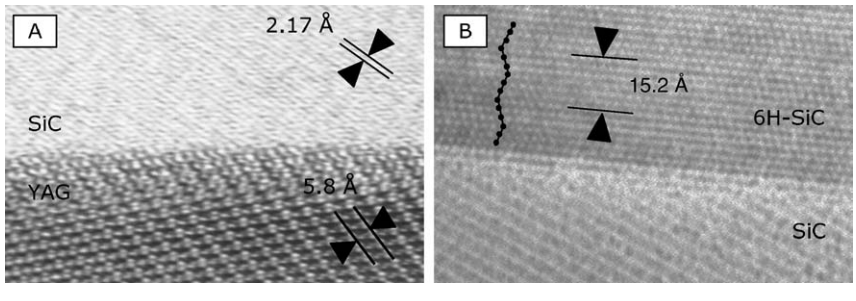

Figure 4 HRTEM images of clean interfaces in the microstructure of SiC ceramics sintered at a temperature of 1950°C; (A) interface between SiC grain and the crystallised secondary YAG phase and (B) interface of two SiC grains.

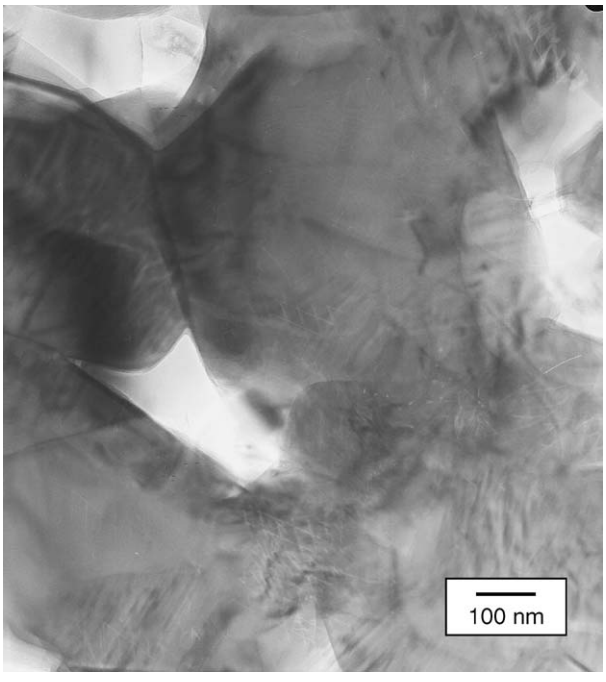

Figure 5 TEM image of the microstructure of a SiC ceramic sintered at a temperature of 1800°C.

the added sintering additives was not detected in the observed part at these magnifications. The round shape of the SiC grains and the strong overlapping of the SiC grain boundaries without clearly pronounced grain boundaries are typically for this SiC ceramic.

Fig. 6 shows an image of a triple point with a secondary phase at a higher magnification. At the top of the image there is a SiC grain with stacking faults. At the bottom, there is a SiC grain covered by an amorphous layer. The phase in the triple point of the SiC grains is the secondary phase which include the sintering additives. Diffraction patterns from this secondary phase reveal its amorphous structure. The observed secondary phase could not be detected in each triple point of the microstructure, like it would be expected for a concentration of 10 vol% of sintering additives. A crystallised secondary phase like the YAG phase in the specimen sintered at a temperature of 1950°C was never observed in this microstructure. This observation is in accordance with XRD measurements which also did not detect a crystallised YAG phase. In this SiC ceramic sintered at 1800°C, the additives and SiO_2 form mainly grain boundary interfaces between the SiC grains. These films exhibit an amorphous structure (Fig. 7). It is generally known that the determination of the thickness of the separating layer is very complicated, but according to the micrograph a thickness of approximately 1 nm is observed, which is consistent with the already mentioned literature.

4. Discussion

The grain boundaries in the microstructure of liquid phase sintered SiC ceramics fired at temperatures of 1800 and 1950°C show several microstructural differences concerning the formation of intergranular amorphous films. SiC ceramics sintered at a temperature of 1800°C have thin separating films with a thickness of approx. 1.0 to 1.5 nm. The HRTEM observations at SiC ceramics sintered at a temperature of 1950°C reveal no amorphous grain boundary films between the SiC grains. There is also no thin amorphous layer between the SiC grains and the crystallised YAG phase in the triple points. From these results it is assumed, that the liquid phase, which is produced at lower temperatures is distributed homogenously around the SiC grains in the entire microstructure after sintering at 1800°C. After sintering at 1950°C the SiC grains have been partially dissolved and reprecipitated, and the amorphous phase was crystallised to the YAG phase.

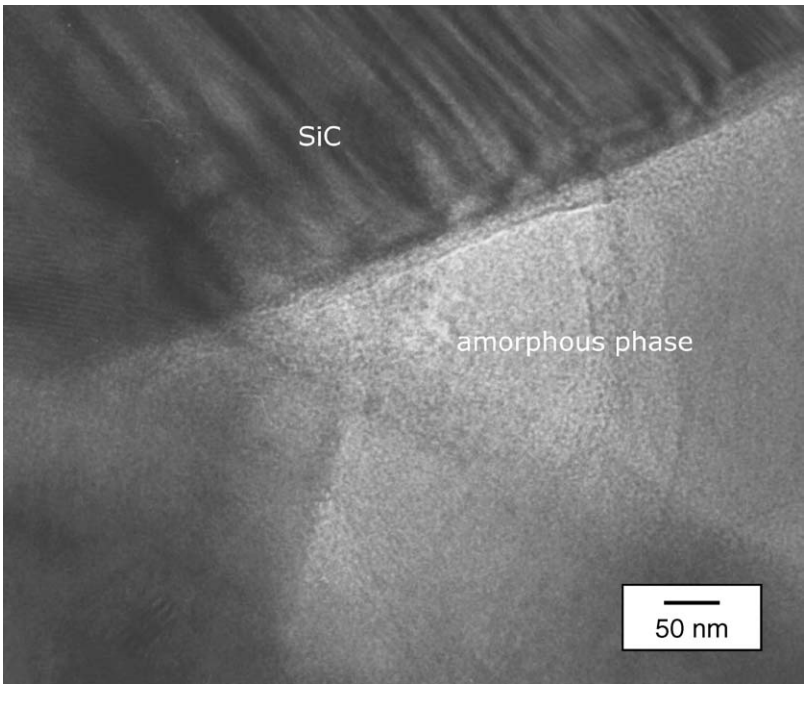

Figure 6 TEM image of secondary phase with an amorphous structure in the microstructure of a SiC ceramic sintered at a temperature of 1800°C.

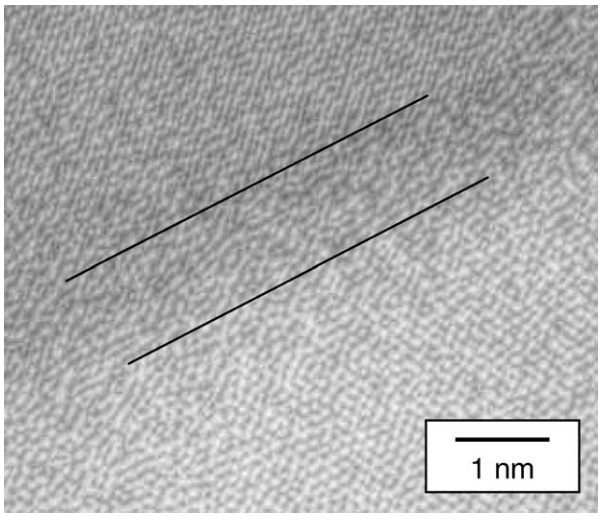

Figure 7 HRTEM image of a SiC ceramic sintered at a temperature of 1800°C with an amorphous layer in the interface of a grain boundary of two SiC grains.

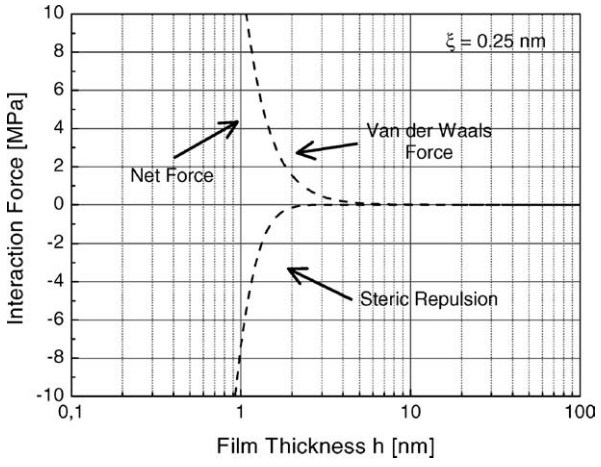

Figure 8 Net Force according to the model of Clarke for the SiC-SiO_2 system with a correlation length of 0.25 nm. No force equilibrium exist for the intergranular film.

The reason for the existence or the absence of the thin amorphous intergranular films in the microstructure of SiC ceramics is up to now not understood in detail, especially if compared to the formation of grain boundary films in silicon nitride ceramics. Clarke [20] was the first who discussed the behaviour of intergranular amorphous films in ceramics based on a model of a liquid SiO_2 layer between SiC grain boundaries and the resulting force equilibrium between attractive and repulsive forces. The attractive force in the force equilibrium is the intermolecular van der Waals force acting between the grains. At higher temperatures the electrical double layer interactions, the solute adsorption and hydrogen bonding can be neglected. Thus, as the repulsive force the steric repulsion has to be taken into account. In the equilibrium state the net force becomes zero. This is expressed in Equation 1 [20], where h is the equilibrium thickness of the intergranular amorphous film. In Equation 1 the external applied pressure and the capillary pressure are zero.

$$\underbrace{\frac{H_{\alpha\beta\alpha}}{6\pi h^3}}_{\substack{\text{van der Waals}\\ \text{force}}} \underbrace{-4\alpha\eta_0^2 \exp\left(\frac{-h}{\xi}\right)}_{\substack{\text{steric}\\ \text{repulsion}}} = 0 \qquad (1)$$

$H_{\alpha\beta\alpha}$, Hamaker constant of a material α separated by a fused material β; h, Film thickness; $\alpha\eta_0^2$, Constant for the measure of the free energy of ordering; ξ, correlation length.

According to Clarke for the system SiC and SiO_2 the Hamaker Constant is 233×10^{-21} J, $\alpha\eta_0^2$ is 100 MPa, and the correlation length is approximately the molecular size of the SiO_4 tetrahedral, which is 0.25 nm. Using Equation 1, the net force can be plotted as a function of the intergranular film thickness h and is shown in Fig. 8. The model shows that there is no stable force balance between the attractive and the repulsive forces for a liquid SiO_2 film between two SiC grains. The model also shows that at any distances the van der Waals attraction is greater than the steric repulsion. An intergranular amorphous film is energetically not stable and the equilibrium thickness of the intergranular amorphous film becomes zero. This suggested model is in good agreement with the HRTEM observations of SiC ceramics sintered at a temperature of 1950°C. At this sintering temperature the grain boundaries at silicon carbide grain interfaces are clean and have no amorphous layer which separates the grains.

The observations at SiC ceramics densified at a sintering temperature of 1800°C are apparently inconsistent with the forecast of the Clarke model for SiC and liquid SiO_2 phase. Clarke assumed a correlation length of 0.25 nm, which is given by the molecular size of the tetrahedral SiO_4. In the model of Clarke the intergranular phase consists of pure SiO_2. But in the investigated ceramic system, there is the possibility of contaminations of the intergranular amorphous film by carbon, aluminum, yttrium, and nitrogen. The carbon can originate from the dissolved SiC in the melt and the graphite furnace, the nitrogen from the contaminated sintering atmosphere, and aluminium and yttrium from the sintering additives. One effect of carbon, which is dissolved in the intergranular amorphous phase can be the increase of the correlation length. In the intergranular amorphous phase the carbon can form SiC_4 tetrahedron with an increased correlation length of approximately 0.31 nm. According to Ackler [21] the correlation length is the most important parameter regarding the intergranular film thickness. The simulation of the net force with an increased correlation length of 0.3 and 0.4 nm, respectively, in the term for the repulsive force is given in Figs 9 and 10. Identical values of the Hamaker constant and of the $\alpha\eta_0^2$ constant were used for these calculations. The extended simulations based on the model of Clarke show that already a small increase of the sensitive parameter ξ will increase the repulsive steric force, and provides a stable force balance in the simulated net force. This enables the formation of an energetically stable intergranular film in SiC ceramics. The stable equilibrium thickness increases with increasing correlation length from 1.2–1.3 nm for a correlation length of 0.3 nm to 2.3–2.4 nm for a correlation length of 0.4 nm.

Therefore, from the physical point of view at a sintering temperature of 1800°C the correlation length is

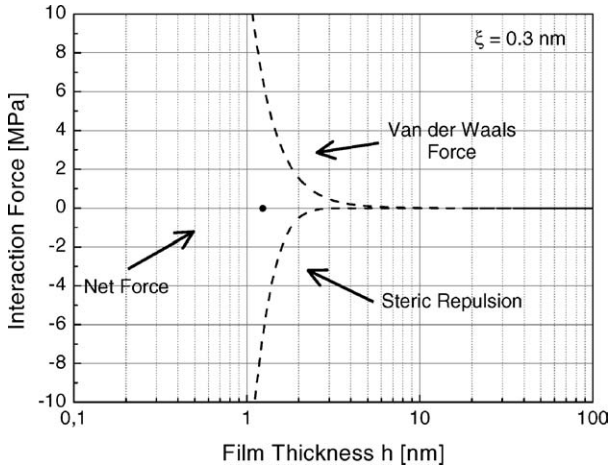

Figure 9 Calculated net force as a function of the intergranular film thickness with an assumption of the correlation length of 0.3 nm for the repulsive steric force. A stabile force balance exists at a film thickness of approximately 1.2 to 1.3 nm.

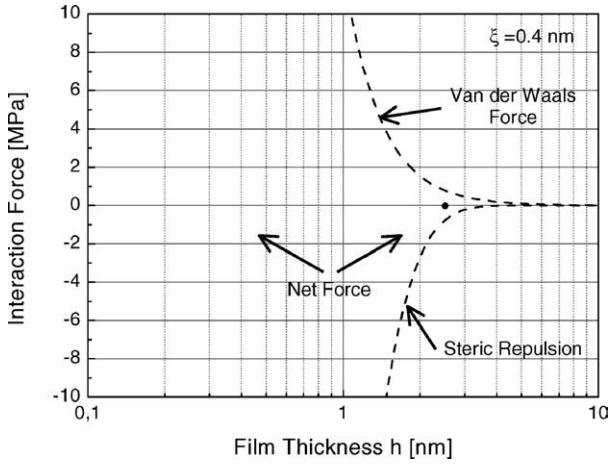

Figure 10 Calculated net force as a function of the intergranular film thickness with an assumption of an increased correlation length of 0.4 nm for the repulsive steric force. Also a stabile force balance exists, but with an increased intergranular film thickness of approximately 2.4 to 2.5 nm.

larger in the liquid phase sintered SiC ceramics, compared to the SiC ceramics sintered at 1950°C. With the assumption of an increased correlation length the model is consistent with the experimental HRTEM observations of the microstructure of liquid phase sintered SiC ceramics sintered at 1800°C. Therefore the applied model is evidence that impurities are present in the intergranular amorphous film of SiC ceramics at a sintering temperature of 1800°C. These impurities are not present at a higher sintering temperature of 1950°C and the correlation length is reduced. Thus the separating intergranular films are no longer energetically stable, because of the lack of a force balance. One explanation for the absence of the impurities in the films at higher temperatures can the enhanced dissolution and reprecipitation process of SiC in the liquid phase at higher temperatures, which results in an incorporation of impurities to the lattice of the SiC grains, particularly in the rim part of the rim/core structure [10]. The second reason for the reduced correlation length and consequently the lower content of impurities can be the increase in the vapour pressure of the liquid phase at higher temperatures which can result in the evaporation of impurities. This also causes a purification of the liquid phase.

From the thermodynamic point of view the different behaviour of the microstructure and the intergranular amorphous film in the two SiC ceramics can also be interpreted by an accelerated decomposition of the SiO_2 film at higher sintering temperatures. The origin of the amorphous film should be the SiO_2 oxidation layer, which covers the surface of each SiC grain. A possible decomposition of the SiO_2 film could be caused by the reaction of the film with the SiC grains to gaseous SiO and CO, given by Equation 2. Furthermore a decomposition of the SiO_2 layer is possible by the reaction of Equation 3 with carbon impurities, which originate from the gaseous atmosphere, the carbonisation of organic components, or the powder synthesis [22].

$$2SiO_2 + SiC \Rightarrow 3SiO + CO \quad (2)$$

$$SiO_2 + 3C \Rightarrow SiC + 2CO \quad (3)$$

Van Dijen [23] could show that additional carbon decomposes SiO_2 during liquid phase sintering of SiC ceramics with the sintering additives of Al_2O_3 and Y_2O_3. The formed liquid phase in this ceramics was free from silica and less weight loss was observed during sintering caused by the reaction of Equation 3. The microstructure of the sintered SiC ceramics showed no amorphous layer between the SiC grains and the secondary phase was completely located in the triple points. A similar behaviour is known from AlN ceramics [24], where oxygen of Al_2O_3 is removed from the microstructure similar to Equation 3.

Finally, it is also possible, that carbon impurities and SiO_2 form a stabile SiOC phase at lower temperatures. This phase is more stable than the SiO_2 phase, because of the character of the bonding and a higher degree of compositional disorder and crosslinking [25]. Up to a sintering temperature of 1800°C it can be assumed that during the sintering and cooling process the stable SiOC phase will not decompose and will remain between the SiC grains. At a temperature of 1950°C the purified silica without carbon impurities is not stable and will decompose during further heat treatment.

5. Conclusion

The observed microstructure of pressureless liquid phase sintered SiC ceramics at 1800 and 1950°C, respectively, can be explained as follows:

(1) The microstructure at a sintering temperature of 1800°C, held for 30 min, is free of crystallised secondary phase and shows intergranular glass films with a thickness of approx. 1 nm separating the SiC grains.

(2) At a higher sintering temperature of 1950°C, held for 30 min, the microstructure is completely different. The secondary phase is crystallised as the $Y_3Al_5O_{12}$ phase. All grain boundaries are clean and have no intergranular amorphous layer.

(3) The existence and the absence of the intergranular amorphous films was explained with an increase of the correlation length of the repulsive steric force in the Clark's force balance model. The increase of the correlation length could be caused by impurities in the intergranular glass films.

(4) Besides the physical reason chemical explanations for the stability of intergranular glass films are also possible. Thus, the SiO_2 phase can decompose in the presence of carbon at higher temperatures.

Acknowledgments

The authors would like to thank the Deutsche Forschungsgemeinschaft (German Research Foundation) and the DAAD (German Academic Exchange Service) for the financial support of this work and Dr. C.-C. T. Yang, Taipei and Mr. M. Albrecht, Erlangen for their experimental support and discussions.

References

1. R. A. ALLIEGRO, L. B. COFFIN and J. R. TINKLEPAUGH, *J. Amer. Ceram. Soc.* **39**(11) (1956) 386.
2. S. PROCHAZKA, "Sintering of Silicon Carbide," General Electric Report 73 CRD 325 (1973).
3. M. OMORI and H. TAKEI, *J. Mater. Sci.* **23** (1988) 3744.
4. S. BOSKOVIC, E. KOSTIC and F. SIGULINSKI, *Sci. Sintering* **23**(3) (1991) 183.
5. M. A. MULLA and D. KRSTIC, *Amer. Ceram. Soc. Bull.* **70**(3) (1991) 439.
6. Y.-W. KIM, M. MITOMO and J.-G. LEE, *J. Mater. Sci. Lett.* **15** (1996) 409.
7. S. K. LEE and C. H. KIM, *J. Amer. Ceram. Soc.* **77**(6) (1994) 1655.
8. N. P. PADTURE, D. C. PENDER, S. WUTTIPHAN and B. R. LAWN, *ibid.* **78**(11) (1995) 3160.
9. M. NADER, F. ALDINGER and M. J. HOFFMANN, *J. Mater. Sci.* **34**(6) (1999) 1197.
10. L. S. SIGL and H. J. KLEEBE, *J. Amer. Ceram. Soc.* **76**(3) (1993) 773.
11. H. YE, V. V. PUJAR and N. P. PADTURE, *Acta Mater.* **47**(2) (1999) 481.
12. L.-M. WANG and W. C. WEI, *J. Ceram. Soc. Jap.* **103**(5) (1995) 434.
13. L. K. L. FALK, *J. Euro. Ceram. Soc.* **17**(8) (1997) 983.
14. *Idem.*, *ibid.* **18**(15) (1998) 2263.
15. T. NAGANO, K. KANEKO and G.-D. ZHAN M. MITOMO, *J. Amer. Ceram. Soc.* **83**(11) (2000) 2781.
16. R. W. CARPENTER, W. BRAUE and R. A. CUTLER, *J. Mater. Res.* **6** (9) (1991) 1937.
17. R. HAMMINGER, H. KRÜNER and W. BÖCKER, *J. Hard Mater.* **3**(2) (1992) 93.
18. H.-J. KLEEBE, *J. Amer. Ceram. Soc.* **85**(1) (2002) 43.
19. I. A. BONDAR and F. YA. GALAKHOV, *Iw. Akad. Nauk SSSR, Ser, Khim.* **7** (1963) 1325.
20. D. R. CLARKE, *J. Amer. Ceram. Soc.* **70**(1) (1987) 15.
21. H. D. ACKLER, "Thermodynamic Calculations and Model Experiments on Thin Intergranular Amorphous Films in Ceramics," Ph.D. thesis, Massachusetts Institute of Technology, Cambridge, MA, 1997.
22. Y.-W. KIM, M. MITOMO and J.-G. LEE, *J. Ceram. Soc. Jap.* **104**(9) (1996) 816.
23. F. K. VAN DIJEN and E. MAYER, *J. Euro. Ceram. Soc.* **16**(4) (1996) 413.
24. C. KÖSTLER, H. BESTGEN, A. ROOSEN and W. D. G. BÖCKER, in "Euro-Ceramics III," edited by P. Duran and J. F. Fernandez (Faenza Editrice Iberica, Spain, 1993) p. 913.
25. Y.-W. KIM and M. MITOMO, *J. Amer. Ceram. Soc.* **82**(10) (1999) 2731.

Received 6 November 2003
and accepted 12 March 2004